ELSEVIER

European Journal of Pharmaceutics and Biopharmaceutics 45 (1998) 137–148

European Journal of Pharmaceutics and Biopharmaceutics

Research paper

Associations of parameters characterizing the time course of the tabletting process on a reciprocating and on a rotary tabletting machine for high-speed production[1,2]

Peter Konkel, Jobst B. Mielck*

Abteilung für Pharmazeutische Technologie, Institut für Pharmazie, Universität Hamburg, Hamburg, Germany

Received 12 September 1996; accepted 22 April 1997

Abstract

A series of modern direct-compression excipients with differing mechanisms of deformation and densification, Karion Instant® Pharma, Vivacel® 200, Cellactose®, Tablettose®, and Parmcompress®, after admixing magnesium stearate, have been tabletted (400 mg, 10 mm flat-faced punches) on an eccentric machine, Fette E XI at 43.6 rpm, and on a rotary machine, Fette PT 2090 at 20, 60, and 90 rpm, to graded maximum forces (3, 5, 10, 15 kN, respectively). Force/time (E XI and PT 2090) and displacement/time (E XI) curves were recorded. From the data on the E XI, parameters of a modified Weibull function, slopes of the Heckel function, quotients of partial areas under the curves, and the differences between times of maximum forces and the respective maximum densifications, t_{diff}, were calculated. From the data on the PT 2090, partial areas under the curves for the upper punch, various quotients of these areas, and the peak-offset times, t_{off}, the times of maximum force relative to the middle of the dwell time, t_{dwell}, were calculated. Close associations were found between the area $A1_{rel}$ during the precompression phase (PT 2090) and the Heckel slope (E XI), between the quotient of partial areas before and after the middle of t_{dwell} (PT 2090) and that of partial areas before and after maximum densification (E XI), and between t_{off} (PT 2090) and t_{diff} (E XI). However, certain materials (e.g. Karion Instant, Vivacel) showed marked deviations in behavior by particular parameters on the two machines. The results from both machines with respect to densification behavior complement one another. © 1998 Elsevier Science B.V.

Keywords: Machine effects; Tabletting parameters; Heckel parameters; Weibull parameters; Area quotients; Relaxation; Compaction speed; Dwell time; Peak-offset time

1. Introduction

In preformulation work with a new drug, initial galenical experiments have to be carried out with very small masses. Yet, the tabletting properties of the material should be known as early as possible to include the necessary excipients in compatibility and stability studies.

In principle, the hydraulic press, the classical small eccentric tabletting machine, and the compaction simulator might be considered for these initial experiments, which then should allow extrapolations to the high-speed production rotary tabletting machine.

While the hydraulic press needs only a small investment and is easily instrumented and handled, the time course of tabletting and the contact time of machine and material under load are highly dissimilar to pharmaceutical tabletting. The compaction simulator, on the other hand, needs a high investment, may be programmed with theoretical displacement/time curves of

* Corresponding author. Abteilung für Pharmazeutische Technologie, Institut für Pharmazie, Universität Hamburg, Bundesstrasse 45, D-21046 Hamburg, Germany. Tel:. +49 40 41233479; fax: +49 40 41236573.

[1] Dedicated with gratitude to Professor emer. Dr.Dr.h.c. Fritz Müller, Bonn, on the occasion of his 70th birthday.

[2] This article is reprinted from *European Journal of Pharmaceutics and Biopharmaceutics*, Vol. 44, No. 3, pp. 289–301 (1997) for the purpose of improved table layout.

0939-6411/98/$19.00
PII S0939-6411(98)00020-4

Table 1

Materials

Material	Symbol	Source	Lot
Cellactose	CE	Meggle, Wasserburg, Germany	D195 L972 A4901
Karion Instant Pharma	KI	E. Merck, Darmstadt, Germany	M 568503
Parmcompress	PA	G. Parmentier, Frankfurt, Germany	91/176 2
Tablettose	TA	Meggle,	D287 L971 A4003
Vivacel 200	VI	J. Rettenmaier, Ellwangen-Holzmühle, Germany	80011073
Magnesium stearate		Riedel-de Haen, Seelze, Germany	91320

any compression machine, but still cannot mimic the complex interaction of the material being tabletted and the machine itself, which reacts to the resistance of the material at least by deformation [1].

Then, the eccentric tabletting machine, a classical piece of equipment in many R and D laboratories, may be considered again:

Single tablets can easily be prepared, the machine is easily instrumented and numerous ways of instrumentation have been proposed and tested [2]. Quasi-static calibration is well documented. Unfortunately, true dynamic calibration has not yet grown beyond the 'punch on punch' experiment, which—owing to the shock-like compression event—should cause responses in the machine very different from pharmaceutical tabletting. The eccentric machine, however, offers only one-sided densification and provides rates of densification far below that of modern production machines.

Therefore, it still seems worthwhile to search for associations among parameters characterizing the tabletting by both an eccentric and a rotary tabletting machine under conditions as similar as possible.

For the force/time and the displacement/time curve from the eccentric machine, several physical and mathematical models are in use, the parameters of which serve to characterize particular phases or the whole tabletting process and are used to assign certain mechanisms prevailing in tabletting, such as elastic, visco elastic, plastic and brittle behavior, to the material.

Data for the compression phase are often approximated by the Heckel function [3]. The complete time course is approximated for instance by physical models, e.g. the visco-elastic deformations of a set of Voigt-Kelvin solids [4], or by mathematical-statistical models, such as the modified Weibull function [5,6a,6b,7] and further developments of this concept [8]. Characteristic points [9] and slopes at particular points of the curve [10], and functions of partial areas under the force/time curve [11] have been used.

From the time course of tabletting in a rotary tabletting machine, functions of partial areas have been derived and used very successfully [12–14]. Besides these areas as a means to characterize mechanisms during phases of tabletting like compression, relaxation, and elastic expansion, the 'peak offset time', t_{off} [15,16], i.e. the time difference between the maximum in pressure and the middle of the dwell time, served as a quantitative indicator for the extent of stress relaxation of the material in the die under constant deformation.

2. Aim of the study

A range of typical pharmaceutical direct-compression materials with well-known prevailing mechanisms of volume reduction, relaxation and elastic deformation during tabletting shall be tabletted under conditions as similar as possible (i) by an eccentric tabletting machine of sturdy construction, widely used and having provided a large body of information on tabletting behavior in the literature, and (ii) by one of the most modern high-speed production rotary machines on the market. The time courses of force and displacement (eccentric machine) and of force shall be evaluated by representative procedures and models, and attempts shall be made to associate such information from the two machines.

3. Materials and methods

3.1. Materials

The materials are shown in Table 1 and were used as received without further classification.

3.2. Methods

3.2.1. Powder-technological properties

Bulk (DIN 53 912) and tap densities (DIN 53 194), as well as true densities by Helium pyknometry (Stereopycnometer SPY2, Quantachrome, NY) were determined in triplicate with samples, equilibrated for at least 10 days at 25 ± 2°C and 50 ± 2% r.h. The confidence limits ($P_{0.05}$) are shown in Table 2.

3.2.2. Mixing of excipients with lubricant

The excipients were mixed with magnesium stearate (Vivacel, Cellactose, Tablettose, Parmcompress: 1% (m/m), Karion Instant: 0.5% (m/m)) in a tumbling mixer (RM 100, J. Engelsmann AG, Ludwigshafen, Ger-

Table 2

Powder technological properties of the excipients in mixture with 1% magnesium stearate (Karion Instant: 0.5%), expressed as confidence limits ($P_{0.05}$) of the means

Material (g/ml)	Bulk density (g/ml)	Tap density (g/ml)	True density (g/ml)
Karion Instant Pharma	0.461–0.468	0.526–0.548	1.488–1.492
Vivacel 200	0.474–0.480	0.553–0.562	1.561–1.565
Cellactose	0.428–0.479	0.511–0.532	1.550–1.553
Tablettose	0.640–0.676	0.718–0.764	1.544–1.548
Parmcompress	0.751–0.768	0.849–0.871	2.334–2.336

many) in a 150 l-stainless steel drum at a filling volume of 20% (Tablettose) to 50% (Cellactose) at 32 rpm for 10 min.

3.2.3. Tabletting machines, conditions, and procedures

For programming and registration of data, for calculation and evaluation of data by least squares approximations, and for graphical representation, the ASYST software package (ASYST Scientific Software System, Vers. 4.0, Macmillan Software Syst., New York) was used throughout.

3.3. Eccentric tabletting machine

An Exacta XI (W. Fette GmbH, Schwarzenbek, Germany) was used. A single punch and die-set with 10.0 mm diameter, flat-faced with a bevelled edge of 0.4 mm, was used at a constant filling depth of 14.0 mm.

3.3.1. Instrumentation

The machine was equipped with strain gauges (6/350 LY 11, Hottinger-Baldwin Messtechnik, Darmstadt, Germany) at the upper and lower pistons, and with two inductive displacement transducers (W 10, Hottinger-Baldwin Messtechnik) mounted at an angle of 45° to the axle of the drive eccentric (5) to eliminate errors due to bending of the upper piston. The signals were amplified (KWS 6/A5 TF, 5 kHz, Hottinger-Baldwin), sampled every 0.667 ms, digitized to 16 bit (DT 2827, Data Translation, Marlboro, MA), and stored in a PC (Sicomp 32-20, Siemens AG, Germany).

3.3.2. Calibration

Quasi-static calibration of the strain gauges in two ranges (0.05–5 kN: load cell K 01301, Gassmann Theiss Messtechnik, Seeheim-Jugenheim, Germany; 5.0–35.0 kN: load cell C4, Hottinger-Baldwin), and calibration of the displacement transducers using gauge blocks according to DIN 861, both were performed and described by Picker [17]. The dynamic determination of the elastic deformation of the punches under load had been investigated previously [7] and was used for correction of the displacement data.

3.3.3. Tabletting procedure

The speed was set to 43.6 tablets/min, about the maximum available. With motor and fly wheel running continuously, a clutch enabled constant conditions with respect to speed and power at the moment where the upper punch face passed the level of the die. Material, 400 mg, (Analytical Balance AE 166/9, Mettler, Greifensee, Switzerland), resulting in maximum lower and upper confidence limits ($P_{0.05}$) of tablet weights of 398.9 and 400.4 mg, respectively, was tabletted to pre-determined maximum forces, F_{max}, at the upper punch. The particular displacements of the upper punch to achieve the particular F_{max} were obtained in preliminary experiments. Fifteen tablets were prepared from each material at each F_{max} in a climatically-controlled room adjusted to 25 ± 2°C and 50 ± 2% r.h.

3.4. Rotary tabletting machine

A PT 2090 (W. Fette GmbH) rotary tabletting machine was used with a central unit for 43 punch and die-sets. The radius of the active rotor (distance of the center of the dies to that of the turret) was 206 mm. Every third position, with one exception, was equipped with flat-faced punches and dies of 10.0 mm diameter with a bevelled edge of 0.4 mm. Fifteen tablets were obtained per revolution. Both precompression rolls were set out of function. The standard motorized feeding unit, filled with >2 kg of material, was used.

3.4.1. Instrumentation

The machine is equipped by the manufacturer with load cells (C 2, Hottinger-Baldwin), positioned between the cases of the axle of each pressure roll and the machine frame. The signals are amplified by 600 Hz carrier-frequency amplifiers (ME 50 S6, Hottinger-Baldwin), the output voltage is used for controlling and documentation. No other amplifiers were allowed to be used. In each experiment, the output voltage (0–10 V) was sampled every 0.1 ms with a time distance of 0.025 ms/channel for a constant length of 1.4 s, digitized and stored as a function of time as described above, resulting in 14 000 points/channel per tablet.

The calculation of data for the distance of the center of

the punch with respect to the perpendicular from the axle of the pressure rolls was enabled by an encoder, registering 3600 electronic pulses per revolution of the die table and in addition one separate pulse for each revolution. Selecting impulses originating closest to the passing of the axle of the punch under that of the pressure roll resulted in a maximum error of 0.05° or 0.18 mm at the circumference of the circle connecting the centers of the dies. At 60 rpm this corresponds to a maximum error of 0.14 ms for the middle of the dwell time.

3.4.2. Calibration

The calibration of the load cells had been performed by the manufacturer (Hottinger-Baldwin) and had to be used.

The force/time curves exhibited a remarkable damped oscillation of roughly 200 Hz after separation of the punch faces from the tablet, which was strongest with Parmcompress, the most elastic material, at high maximum force, F_{max} (Fig. 1). While the characteristic frequency of the load cell itself is documented by the manufacturer to be about 14 kHz ± 15%, the masses coupled to it may reduce this frequency considerably. They are estimated at being about 18 kg. From the known minimum edge height, s_{min}, of a material at a known F_{max} in the eccentric machine, and that set for the rotary machine with the same material, the elastic spring constant D for the swinging system may be estimated from $D = F_{max}/s_{min}$ to about 133 kN/mm. Then the characteristic frequency of this combination of a damped spring and a pendulum may be estimated as ~430 Hz, which is not far from the 200 Hz observed. A model calculation of the effect of this system on the force/time curve in the rotary machine [18] principally explained both the increase in force during the dwell time, and the damped oscillation after separation of punch face and tablet, observed in extreme cases. Since it is not justified to analyze the oscillation in more detail, e.g. by Fourier analysis, because of the interactions of the machine and the respective material at the respective tabletting conditions, the descending force/time curves were cut off at the first time point, where the force reached zero.

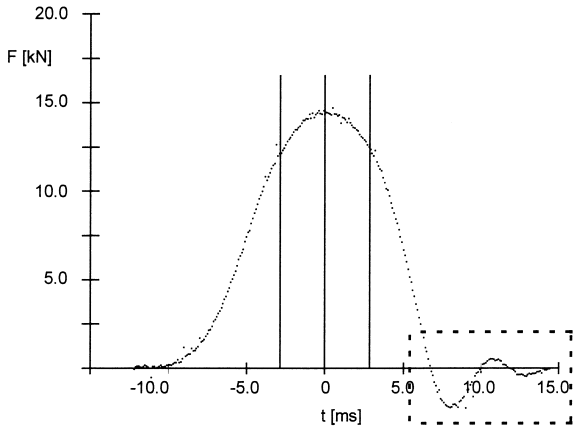

Fig. 1. Rebouncing of the force signal for the upper punch of the Fette PT 2090 rotary machine after separation of the punch from the surface of the tablet (tabletting of Parmcompress at 90 rpm and 15 kN).

3.4.3. Plausibility check

In order to check the plausibility of the data obtained in light of the lack of dynamic calibration of the force-recording systems at the location of the tabletting event, i.e. the punch faces, rough comparison is made to the data obtained by Vogel [19] who used a range of materials very similar in tabletting behavior, and another modern rotary machine, a Korsch PH 230 (Korsch Maschinenfabrik, Berlin, Germany), equipped with identical punches and instrumented with strain gauges at the arms holding the pressure rolls, which had been carefully and completely calibrated using a piezo-electric load washer between a punch set, and which was run under comparable conditions as in this study. Table 3 compares the experimental conditions in the two studies. For comparison, the quotients of the partial areas under the force/time curve of the second half ($A3$) and the first half ($A2$) of the dwell time are used (see Section 3.7.2.1 for calculation of the areas). Table 4 lists the values for the quotients obtained. Considering the differences in the compression phase, caused by different diameters of the pressure rolls, and in the dwell time, which is ~20% longer in the present study at 20 rpm, the correspondence in the data is judged as good, which contributes to the validity of the data presented here.

3.4.4. Tabletting procedure

The tabletting machine had to be run under full computer control. The ‘maximum’ pressure was adjusted to the desired values by exactly vertical adjustment of the position of the pressure rolls to achieve maximum forces of 3, 5, 10, and 15 kN, respectively. For each condition in ‘maximum’ force, the speed of the machine was set to 20, 60, and 90 rpm, respectively. For each material at each F_{max}, 13–17 force/time curves were obtained at 20 rpm, 55–59 at 60 rpm, and 87–89 at 90 rpm.

Table 3

Comparison of conditions for tabletting on a Korsch PH 230 [19] and a Fette PT 2090 rotary tabletting machine, both using Euronorm B punches (diameters: flat head area 10 mm, punch tip 10 mm, flat faced, bevelled edge)

Machine	Korsch PH 230	Fette PT 2090
D_{ar}^{a} (mm)	195	412
D_{pr}^{b} (mm)	200	250
Turning speed (rpm)	50	20
Punch speed (mm/s)	510	432
Tablet weight (mg)	Unknown	400
$F_{u,max}^{c}$ (kN)	10	10

[a]Active rotor diamater, i.e. the diameter of the circle described by the center of the dies.
[b]Diameter of the pressure rolls (no pre-pressure used).
[c]Maximum pressure at the upper punch.

Table 4

Quotients of areas under the force/time curve during the second half (*A*3) and the first half (*A*2) of the dwell time for tabletting of various direct compression excipients, mixed with 1% (m/m) magnesium stearate (exception: Karion Instant, Fette PT 2090: 0.5%) under the respective conditions of Table 1

Material	Machine	
	Korsch PH 230	Fette PT 2090
Avicel PH101	0.923	—
Vivacel 200	—	0.935
Cellactose	0.910	0.935
Karion Instant	0.877	0.895
Tablettose	0.929	0.955
Bekapress D2	0.952	—
Parmcompress	—	0.965

Data for the Korsch PH 230 from [19].

3.5. Time course for volume reduction in comparison

For comparing punch speeds and times at certain levels of displacement for the two machines, theoretical displacement/time curves were calculated for both machines with empty dies. This seemed to be appropriate for an estimate, even for the eccentric machine, since from the rotary tabletting machine no measured data on displacements were available.

For the eccentric machine, the equation of Führer [20], for the rotary machine, the equation by Hoblitzel and Rhodes [21], were used for the calculations. The results for both machines are depicted in Fig. 2.

The authors [21] also provided an equation for calculating the length of the dwell time, t_{dwell}.

3.6. Tablet properties

3.6.1. Tablet weight

The confidence limits ($P_{0.05}$) for the tablet weight (mg) from the eccentric machine over all materials ranged from 398.5 to 400.5, for the rotary maschine the respective numbers were 394.5 (Parmcompress at 20 rpm and 5 kN) to 405.3 (Cellactose at 90 rpm and 15 kN), but were generally much smaller even for the rotary machine. Tablet heights and the crushing strength for the tablets were determined by a diametral compression test (TBH 28, Erweka, Heusenstamm, Germany) 10 days after production and storing at 25 ± 2°C and 50 ± 2% r.h. ([18], data not shown).

3.7. Calculation of parameters

3.7.1. Eccentric machine

3.7.1.1. Heckel-slope K. The data recorded in the compression phase were divided into ten parts, and by linear regression of the Heckel number, $\ln(1/(1 - D_{rel})) = -\ln \varepsilon$, with ε as porosity, on force at the upper punch, the slopes of these ten sections were calculated. Then, starting with the section with the smallest slope, a range of sufficient linearity was found by stepwise inclusion of more data until they exceeded the 6-fold mean SD of the expanding section around its regression line. This slope was taken as the Heckel parameter K (MPa^{-1}). This procedure seemed sufficient in light of the extremes in the extension of 'linear' regions observed (Fig. 3), although linear regressions in such cases have been legitimately questioned [22]. From the values for the number of compressions performed at the four maximum forces, the confidence limits of the means ($P_{0.05}$) for each condition were calculated. The results, expressed as ranges, are shown in Table 5.

3.7.1.2. Weibull parameters γ and β. For an approximation of the pressure/time curve, calculated from the force/time curve and the area of the punch face, by a modified Weibull function, a range of data to be used is selected by applying the following criteria [7]:

t_{anf} = time, where p exceeds 1 MPa

t_{end} = time, where p falls below 1.5 MPa

The modification of the Weibull function proposed by Dietrich and Mielck [5], which needed three parameters, α, β, γ, and normalization of the data and mirroring at the ordinate, leading to relative values for $t_{anf} = 100$, $t_{end} = 0$, $p_{max} = 100$, was simplified by eliminating the parameter α and using the following form of the Weibull function:

$$p(t) = p_{max} \cdot ((t_{end} - t)/(t_{end} - t_{max}))^{\gamma} \cdot e^{1-((t_{end}-t)/(t_{end}-t_{max}))^{\gamma}} \quad (1)$$

where t is the time variable, $p(t)$ is the pressure at time t, p_{max} is the maximum pressure, t_{end} is the time, where p first falls below 1.5 Mpa, and t_{anf} is the time, where p first exceeds 1 MPa for 6.65 ms.

The parameters γ, t_{max} and p_{max} are approximated by a Gauss–Newton method implemented in the ASYST soft-

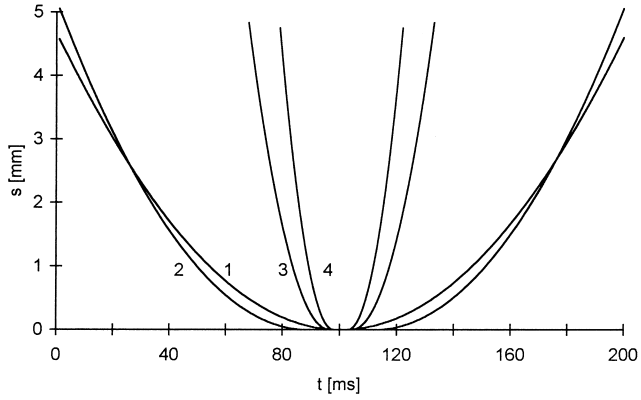

Fig. 2. Displacement/time curves, calculated for the upper punches and empty dies, for the eccentric (43.6 rpm, curve 1) and the rotary tabletting machine (20 rpm, curve 2; 60 rpm, curve 3; 90 rpm, curve 4).

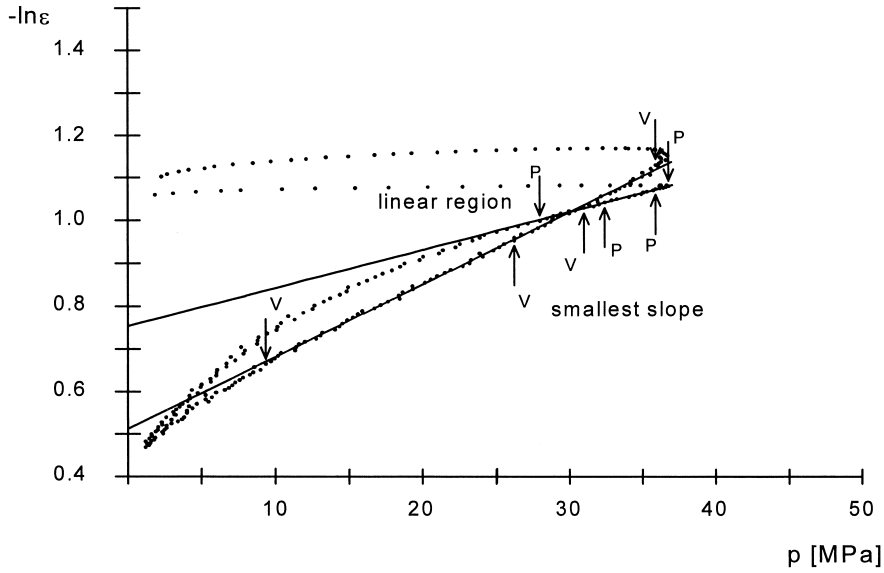

Fig. 3. Heckel plots (–ln ε versus p) from tabletting on the eccentric machine Fette E XI at 43.6 rpm as examples for extreme curve forms: Vivacel 200 (V) at 3 kN and Parmcompress (P) at 3 kN maximum force. Regions with smallest slopes and expanded linear regions are indicated.

ware package. The parameter β is then calculated from Eq. (2):

$$\beta = 100 * (t_{end} - t_{max}) / (t_{end} - t_{anf}) \quad (2)$$

The results for β and γ are expressed as upper and lower confidence limits ($P_{0.05}$) of the means of the individual parameters for the curves recorded [18]. These parameters will be plotted later (see Section 4.2.2) against maximum relative density, $D_{rel,max}$. The latter was calculated from the maximum displacement, corrected for elastic deformation of the machine and punches, which lead to the maximum apparent density, and from the true density.

3.7.1.3. Areas under under the compression and decompression curves. The area under the force/time curve is calculated using a 1/3 Simpson rule (ASYST) and divided at the measured maximum displacement, s_{max}, or minimum edge height under load (Fig. 4). This is in contrast to the method of Emschermann and Müller [11], who divided the area at the measured F_{max}. The area under the compression curve, *A*I, thus includes the increase in force caused by densification and decrease in force at diminishing rates of densification by relaxation. This should more closely resemble the conditions during tabletting with a rotary machine including the compression phase and the first half of the dwell time. The area under the decompression curve, *A*II, should be a measure predominantly of fast elastic expansion. In Fig. 5, the quotients of *A*II and *A*I are plotted as a function of $D_{rel,max}$.

3.7.1.4. Time difference between F_{max} and s_{max}, t_{diff}. The differences, t_{diff}, between the times for the maximum force, F_{max}, and the maximum displacement, s_{max}, were directly read from the recorded data, corrected for elastic

Table 5

Slopes, K (MPa^{-1}) $* 10^{-2}$, of the Heckel function, –ln ε, expressed as confidence limits ($P_{0.05}$) of the mean, obtained on the eccentric tabletting machine Fette E XI (for experimental conditions, see Section 3.3)

Material	Maximum force, F_{max} (kN)			
	3	5	10	15
KI	1.48–1.51	1.21–1.23	1.01–1.02	0.91–0.92
VI	1.66–1.68	1.46–1.47	1.13–1.14	0.87–0.90
CE	1.29–1.33	1.02–1.03	0.76–0.77	0.65–0.65
TA	1.12–1.15	0.82–0.84	0.57–0.58	0.48–0.49
PA	0.90–0.93	0.60–0.62	0.34–0.35	0.25–0.25

Symbols as in Table 1.

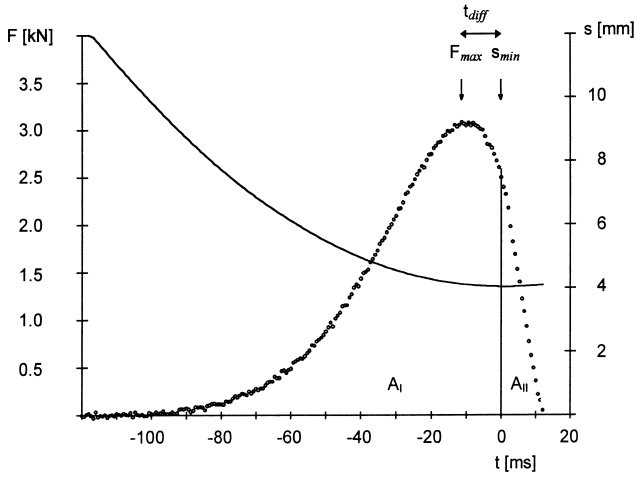

Fig. 4. Force/time curve from the eccentric machine Fette E XI and indication of division into characteristic areas, *A*I and *A*II, and definition of the time difference, t_{diff}, between maximum force and maximum densification (Karion Instant at 43.6 rpm).

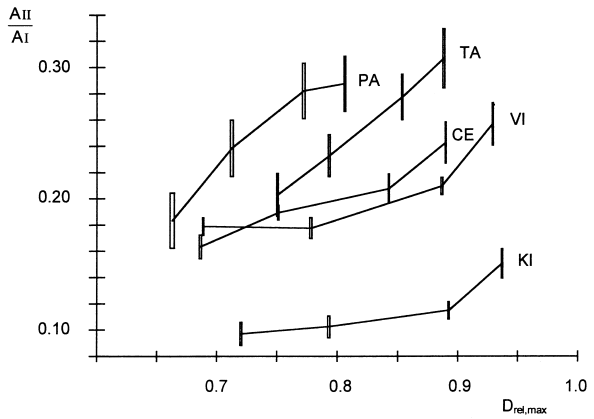

Fig. 5. Quotient of the partial areas *A*II and *A*I, plotted against the calculated maximum relative density, $D_{rel,max}$, for different materials (symbols see Table 1) tabletted on the Fette E XI to graded maximum forces.

deformation. As above, the upper and lower confidence limits of the means ($P_{0.05}$) were calculated and collected in Table 6.

3.7.2. Rotary machine

3.7.2.1. Partial areas under the force/time curve

The area under the force/time curve was calculated as described above. The particular t_{dwell} time was calculated [21]. The area was then divided at the impulse indicating the exact vertical position of the punch axle under the center of the pressure roll. The resulting partial areas, named ($A1 + A2$) and ($A3 + A4$), respectively, were divided once more at the beginning and the end of t_{dwell}, respectively, as proposed by Koch and Schmidt [13], resulting in the areas *A*2 and *A*3 (Fig. 6). Since these areas might be compared with the partial areas under the force/time curve from the eccentric machine [11], the increase in sensitivity of this method was not enhanced, as was proposed by Vogel and Schmidt [14], by subtracting from the areas *A*2 and *A*3 the rectangles under the minimum compaction force during t_{dwell}, thus leading to reduced areas *A*5 and *A*6, respectively. It should be mentioned that there are no sharp edges between the curved and the flat portions of the punch heads in order to avoid damage to the pressure roll, when the punch head hits the roll. Using a slide rule, the diameter of the flat portion was read as 10.0 mm; this value was used in all calculations.

Values for partial areas and quotients of partial areas are expressed, as above, as the confidence range ($P_{0.05}$) of the respective mean value calculated for the number of curves used.

3.7.2.2. Peak-offset time, t_{off}. The difference in time between the maximum force at the upper punch and the middle of t_{dwell}, t_{off}, was read from the recorded force data, and t_{dwell} calculated as above. The confidence ranges ($P_{0.05}$) were large. The data are shown in Table 7.

4. Discussion

4.1. Time course of volume reduction

The main differences in the time course of volume reduction between an eccentric and a modern rotary tabletting machine lay in the rate and in the time during which the material is under high stress relative to the total contact time (Fig. 4). It should be noted, that in spite of the gross similarity of the rate of densification of the PT 2090 at 20 rpm to that of the E XI at 43 rpm by the upper punches, in the rotary machine the densification occurs at equal rate from two sides, in effect therefore at twice the rate. Further, from the change in rate with displacement of the upper punch, it is obvious that the PT 2090 reduces the volume very fast and then provides a relatively long time for relaxation; the E XI causes the punch face to decelerate more gradually and should cause less overriding of irreversible deformation mechanisms, thus allowing earlier relaxation.

4.2. Selected parameters from the eccentric machine

4.2.1. Slope of the Heckel plot, K

As has been reported consistently [22], the Heckel slope obtained under load (‘at pressure’) or its reciprocal, often called mean yield pressure, should be regarded as a constant describing only the tendency or readiness of compressed material to undergo deformation in general. Typical Heckel plots are shown at low maximum upper punch force for the materials showing extremes in behavior, i.e. Vivacel and Parmcompress, in Fig. 3. An extended non-linear part at low pressure often indicates fragmentation, (e.g. Parmcompress), while a long quasi-linear portion (e.g. Vivacel) points to prevailing plastic flow, in combination with elastic deformation. The Heckel slopes will be used as fairly non-specific test parameters later.

4.2.2. Weibull parameters β and γ

The form of the pressure/time function is characterized mainly by the parameter γ, high values indicating high resistance against densification and—in a plot of relative pressure against time—a late and steep increase in pressure

Table 6

Time differences, t_{diff} (ms), between the time of maximum force, F_{max}, and maximum densification for tabletting different materials (symbols as in Table 1) on the eccentric tabletting machine Fette E XI to graded maximum forces, expressed as confidence limits ($P_{0.05}$) of the mean

Material	Maximum force, F_{max} (kN)			
	3	5	10	15
KI	11.0–12.2	10.7–12.1	10.5–11.4	9.34–10.7
VI	7.83–9.60	7.48–8.89	6.78–7.80	5.63–6.55
CE	6.75–8.01	7.06–7.97	6.67–7.82	6.42–7.28
TA	4.65–6.20	4.64–6.13	4.95–6.08	4.66–5.75
PA	2.72–4.04	2.20–3.85	3.08–4.30	4.32–5.20

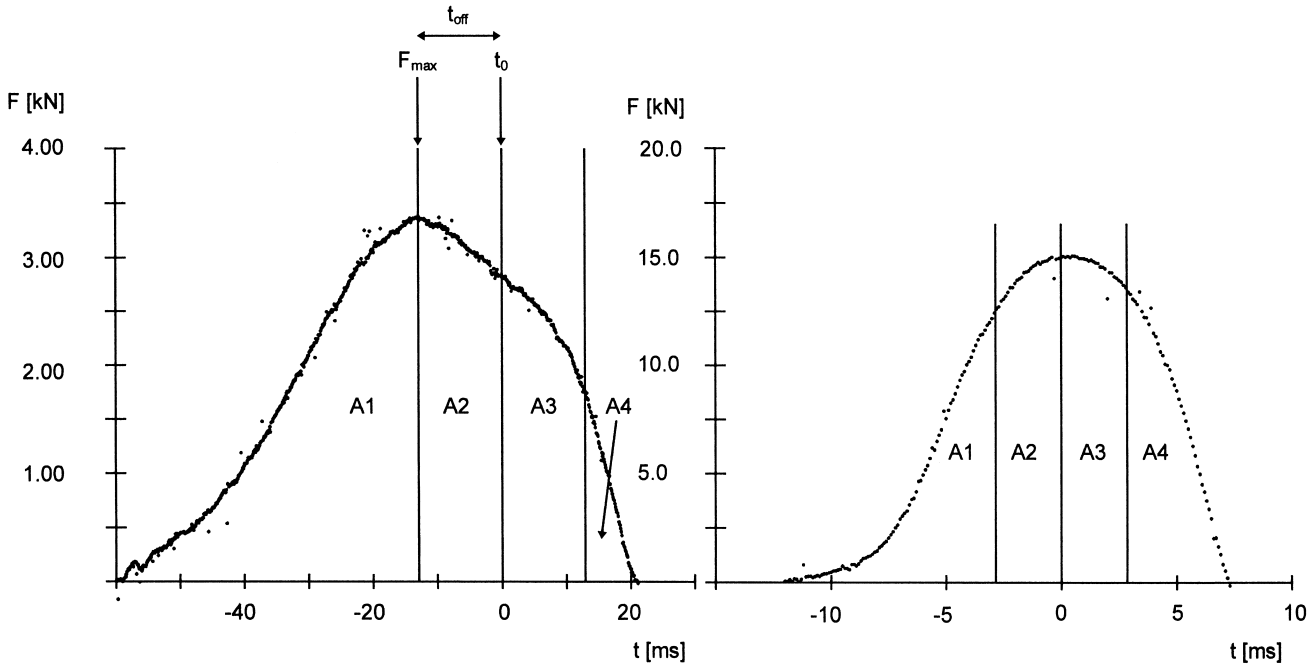

Fig. 6. Indication of the method to divide the area under the force/time curve from the Fette PT 2090 rotary machine according to Schmidt and coworkers, and definition of the peak-offset time, t_{off} (at time 0 the axles of the punches pass the vertical line between the centers of the pressure rolls). (a) Karion Instant at 20 rpm, F_{max} = 3 kN (b) Parmcompress at 90 rpm, F_{max} = 15 kN.

with time. However, possibly different mechanisms of densification under certain conditions may lead to similar pressure/time profiles and identical values for γ. When γ is plotted against $D_{rel,max}$, (Fig. 7) an increase in γ originates

Table 7

Peak-offset times, t_{off} (ms), of the time of maximum force, F_{max}, from the middle of the dwell time during tabletting of different materials (symbols as in Table 1) on the rotary tabletting machine Fette PT 2090 to graded maximum forces, at graded rotation speeds, expressed as confidence limits ($P_{0.05}$) of the mean

Material	F_{max} (kN)	Rotation speed (rpm)		
		20	60	90
KI	3	–15.9 to –12.2	–3.97 to –3.49	–2.13 to –1.82
	5	–13.6 to –11.4	–3.58 to –3.28	–1.90 to –1.73
	10	–9.56 to –6.63	–2.54 to –2.12	–1.59 to –1.41
	15	–8.85 to –3.62	–1.64 to –0.89	–0.92 to –0.69
VI	3	–16.6 to –10.4	–4.00 to –3.18	–1.79 to –1.46
	5	–12.1 to –8.94	–2.76 to –2.29	–1.97 to –1.76
	10	–7.11 to –4.13	–1.52 to –1.12	–0.56 to –0.35
	15	–4.37 to –0.83	–0.59 to +0.10	–0.01 to +0.32
CE	3	–13.6 to –6.40	–3.23 to –2.51	–1.82 to –1.49
	5	–9.27 to –4.93	–2.45 to –1.81	–1.54 to –1.30
	10	–5.96 to –2.26	–1.55 to –1.15	–0.71 to –0.51
	15	–3.72 to –0.48	–1.04 to –0.38	–0.19 to +0.21
TA	3	–7.77 to –3.32	–2.07 to –1.18	–1.50 to –1.16
	5	–8.17 to –2.75	–1.63 to –0.98	–1.31 to –0.89
	10	–5.67 to –2.77	–1.06 to –0.69	–0.18 to –0.04
	15	–7.40 to –2.80	–0.73 to +0.02	–0.28 to +0.07
PA	3	–3.49 to +1.12	–0.74 to –0.11	–0.36 to +0.07
	5	–2.72 to +0.92	–0.66 to –0.19	+0.11 to +0.34
	10	–2.90 to –0.22	–0.10 to +0.25	+0.20 to +0.34
	15	–2.33 to +3.61	+0.06 to +0.83	+0.19 to +0.53

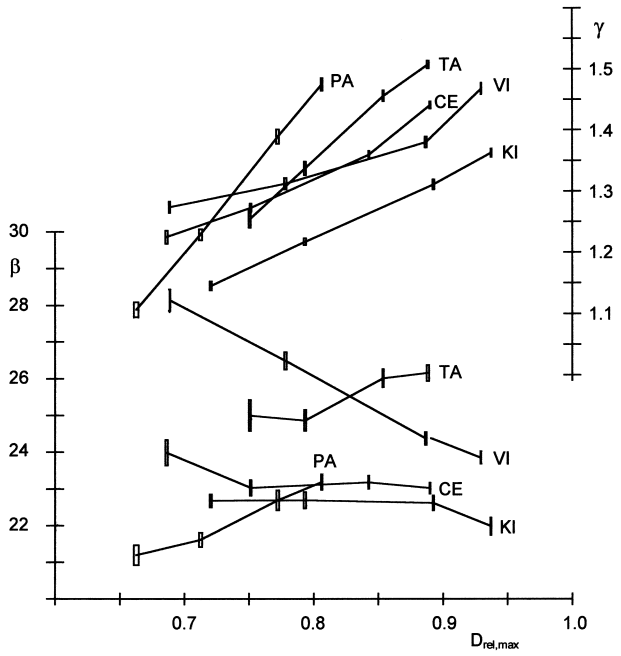

Fig. 7. Weibull parameters γ (right ordinate) and β (left ordinate) for tabletting different materials (symbols see Table 1) at 43.6 rpm to graded maximum pressures, plotted against calculated maximum relative densities, $D_{rel,max}$; confidence limits ($P_{0.05}$) of the means.

from a steeper pressure/time curve (Tablettose, Parmcompress) which points to brittle fracture. The materials that are easily densified, most probably by plastic flow, i.e. Vivacell and Karion Instant, may thus be differentiated from the former, and Cellactose seems to behave plastically, too.

The parameter β (Fig. 7) corresponds to a deloading time—in absolute values, it increases with $D_{rel,max}$ more for Parmcompress and Tablettose, than for the other materials; when relative times are considered, it even decreases, slightly with Cellactose and Karion Instant, more pronounced with Vivacel; this is caused by the increasing contact time.

4.2.3. Quotients of areas under the force/time curve

Generally, the quotient increases with $D_{rel,max}$ (Fig. 5), and with p_{max} accordingly. However, with plastic materials, a noticeable increase, pointing to developing elasticity, is observed only at high densification, while this occurs at low ones with Parmcompress, levelling off at high densification. Karion Instant exposes much lower quotients than Vivacel. Tablettose shows intermediate values and linear dependency in the region investigated. These quotients will be associated later with corresponding quotients from the rotary machine.

4.2.4. t_{diff}

The occurence of the maximum force before the maximum of volume reduction can only be attributed to relaxation by plastic flow. Both the differences in time and in displacement have been proposed to be a measure of relaxation by Schierstedt and Müller [9], an interpretation, which was expanded later by Ho and Jones [23]. Although the data (Table 6) show broad confidence intervals, owing to the rather small time differences, the materials can clearly be differentiated: Karion Instant exposes the maximum, Parmcompress the minimum in plastic deformation. With plastic materials, the parameter decreases with increasing maximum force, indicating an increase in elasticity. In contrast, the parameter values for Parmcompress increase with maximum force, pointing to an increase in time-dependent deformation under high load. It is interesting to note that there is only little difference between Vivacel and Cellactose; probably the small proportion in cellulose in the latter [24] dominates the deformation process.

4.3. Selected parameters from the rotary machine

4.3.1. Partial areas under the force/time curve

In accordance with the large body of experience collected by Schmidt and his coworkers [12–14], the ratios of partial areas after and before the middle of t_{dwell} clearly indicate the extent of irreversible deformation of the material under load. With a perfectly elastic body, the force/time curve should be symmetrical, while a visco-elastic material will deform with time subsequent to the fast volume reduction in the 'precompression' phase preceding t_{dwell}. During t_{dwell}, the volume is nearly held constant, resulting in a decrease in force at the punch. Fig. 6a, b represent extremes in the answer of a material to densification, in mechanisms of deformation, and in tabletting conditions. The respective partial areas and quotients are depicted in Figs. 8–11.

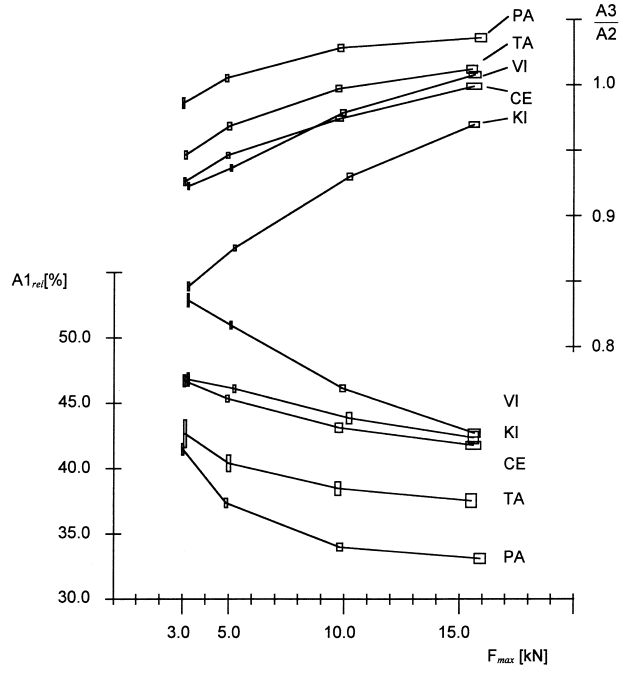

Fig. 8. Relative area, $A1_{rel}$, during the precompression phase (left ordinate), and area quotient, $A3/A2$, (right ordinate) under the force/time curve as functions of F_{max}, obtained from tabletting different materials (symbols see Table 1) on the rotary machine Fette PT 2090 at 60 rpm to graded maximum forces; confidence limits ($P_{0.05}$) of the means.

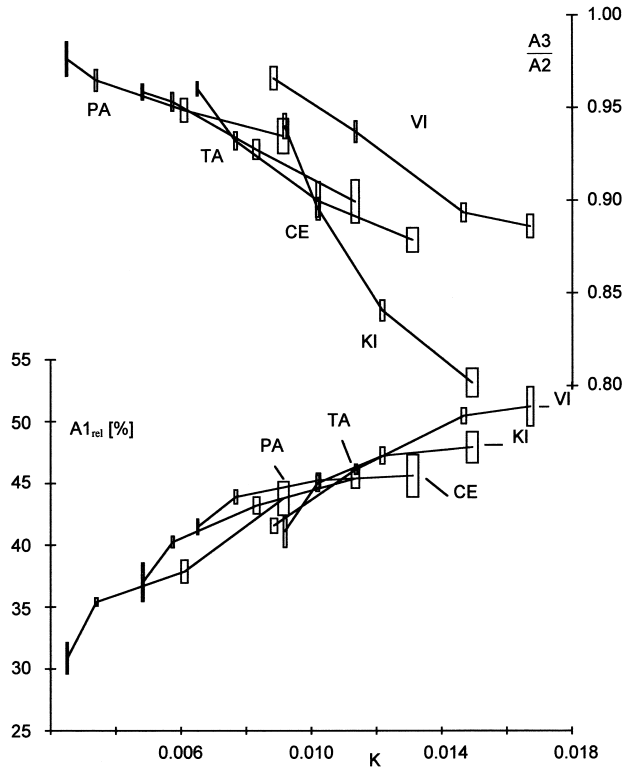

Fig. 9. Relative area, $A1_{rel}$, during the precompression phase (left ordinate), and area quotient, *A*3/*A*2, (right ordinate) under the force/time curve from the rotary machine correlated to the Heckel slope, *K*, calculated from data from the eccentric machine. Data for tabletting different materials (symbols see Table 1) on the Fette PT 2090 at 60 rpm and on the Fette E XI at 43.6 rpm to graded maximum forces; confidence limits ($P_{0.05}$) of the means.

4.3.1.1. Quotient (A3 + A4)/(A1 + A2). With respect to the extent of symmetry of the curves for all materials under all conditions tested, judged from these quotients (results not shown [18]), an order of Parmcompress > Tablettose > Cellactose > Vivacel-Karion Instant is observed. Even with more brittle materials this quotient clearly depends on tabletting speed, which points to an increase in elasticity, either caused by entrapped air or by increased dynamic deformation of the machine.

4.3.1.2. Quotient A3/A2. More sensitive and informative is the parameter calculated from the areas *A*3 and *A*2 (Fig. 6, [13]). Fig. 8 depicts the dependence of this parameter on F_{max}. As expected, Parmcompress and Karion Instant show extreme values. Vivacel seems to creep only moderately under load. However, the elastic deformation also of the machine increases with F_{max} and decreases with relaxation of the material. This may be an indication, that the effect of the proportion of 'reformation' of the machine during t_{dwell} is not constant but interacts with the effects caused by the material. This should also hinder the extraction of information on the elastic properties of the materials from the quotient of the partial areas *A*4/*A*1 (see also Section 4.4.4).

4.3.1.3. $A1_{rel}$. Another parameter of use may be the area during the compression phase, preceding t_{dwell}, named *A*1 in Fig. 6, relative to the area of the rectangle originated by the time and force at the beginning of the dwell time. These areas, obtained at 60 rpm as an example, are plotted against F_{max} in Fig. 8. They seem to be able to clearly differentiate materials according to their readiness for densification, however without giving insight into mechanisms. Vivacel exhibits a very high value at low F_{max}, even compared to Karion Instant.

4.3.2. Peak-offset time

Usually, the dwell time is believed to provide constant deformation, deduced from the geometry of the pressure roll and the punch heads, but the values reported for such peak-offset time still raise some questions. At constant deformation, force exerted on the punch by the material can only decrease or remain constant and thus should result in times for the maximum force identical with the beginning of t_{dwell}, at the latest; t_{off} then will be equal to or greater than one half of t_{dwell}. However, the force measured normally increases further after the beginning of t_{dwell}, and thus, the values reported are smaller than one half of the latter (Fig. 6), [14]. In fact, Dwivedi et al. [16] have fixed the middle of t_{dwell} (t_{off} = 0) by the time of F_{max} observed for Emcompress at high pressure. Obviously, the densification proceeds further during t_{dwell}, which may be superceded by relaxation with highly plastic materials and may not be detected. Tilting of the punches when they reach and leave the pressure roll might cause further densification [13].

Values for t_{off} close to half of t_{dwell} (calculated: 23.3 ms at 20 rpm, 7.8 ms at 60 rpm, and 5.2 ms at 90 rpm) were found for highly plastic materials, at low F_{max} and at low turning speed (Table 7); t_{off} decreases with decreasing readiness for densification, increasing F_{max}, and increasing turning speed.

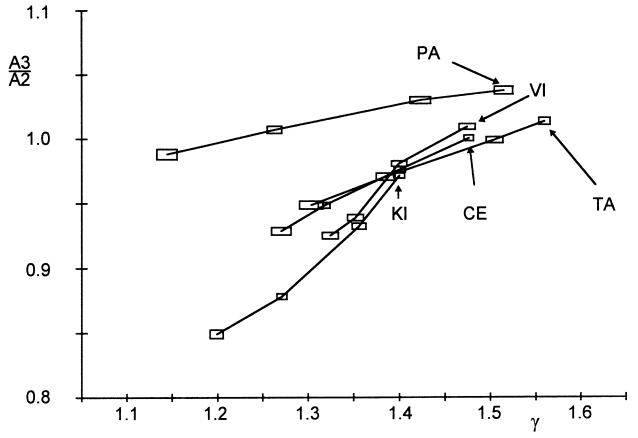

Fig. 10. Area quotient, *A*3/*A*2, for the force/time curve during the dwell time on the rotary machine correlated to the Weibull parameter γ, calculated from data from the eccentric machine. Data for tabletting different materials (symbols see Table 1) on the Fette PT 2090 at 60 rpm and on the Fette E XI at 43.6 rpm to graded maximum forces; confidence limits ($P_{0.05}$) of the means.

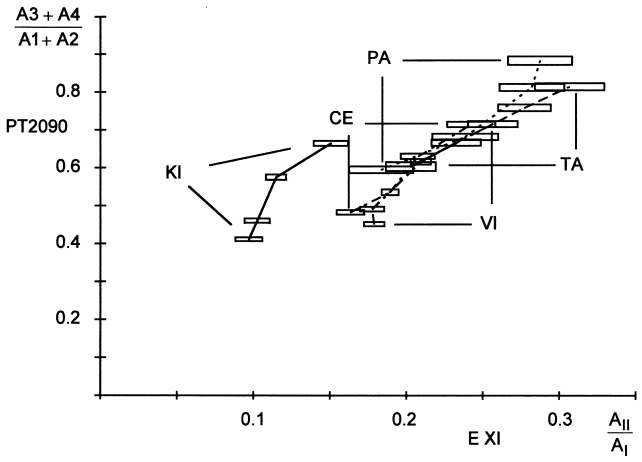

Fig. 11. Area quotient, (*A*3 + *A*4)/(*A*1 + *A*2), for the force/time curve of the rotary machine, divided at the middle of the dwell time, correlated to the area quotient, *AII*/*AI*, for the force/time curve of the eccentric machine, divided at the time of maximum densification. Data for tabletting different materials (symbols see Table 1) on the Fette PT 2090 at 60 rpm and on the Fette E XI at 43.6 rpm to graded maximum forces; confidence limits ($P_{0.05}$) of the means.

4.4. Associations among selected parameters from both tabletting machines

4.4.1. Partial area $A1_{rel}$ and Heckel slope

There is a surprisingly linear relation of the partial area $A1_{rel}$ and the slope of the Heckel function 'at pressure', *K*, (Fig. 9). However, as has been pointed out, both parameters characterize the readiness of the materials for deformation and do not allow assignements of mechanisms of deformation without further evidence.

4.4.2. Area quotient A3/A2 and Heckel slope

Apparently, there is a correlation between the area quotient during the dwell time and the slope of the Heckel function 'at pressure', *K*, (Fig. 9), however, this holds mainly for the more brittle materials. While the values for *K* for Karion Instant and Vivacel do not widely differ, Vivacel undergoes much less relaxation than Karion Instant, as shown by the area quotients especially at high load. This may at least partially be explained by the combination of elastic and plastic deformation, contained in the values for *K*.

4.4.3. Quotient A3/A2 and Weibull parameter γ

While area quotients as parameters obtained from data of the rotary machine contain information about the position of the punches and thus are bound to certain sections of the force/time curve, the parameter γ of the Weibull function is completely independent of displacement and only describes the form of the total force/time curve. As can be seen in Fig. 10, within one material a correlation seems to exist, since both parameters increase with increasing F_{max}. However, in an attempt to correlate the parameters at a certain F_{max}, no correlation can be detected.

4.4.4. Quotient A4/A1 and Weibull parameter β

Similarly, no correlation exists between the area quotient *A*4/*A*1 (data not shown, [18]) and the Weibull parameter β, although both parameters contain information on the fast elastic recovery during tabletting. Probably, the information on fast elastic recovery of the material during the time following t_{dwell} is dominated by the marked elastic behavior of the PT 2090 (see Section 3.4.2), which is supported by analysis of the respective data for absolute, fast elastic recovery within the die [18].

4.4.5. Quotient (A3 + A4)/(A1 + A2) and AII/AI

A close correlation seems to exist (Fig. 11) between the quotients of areas under the force/time curves from both machines, which are calculated for the respective time courses up to the maximum densification (E XI) and the middle of t_{dwell} (PT 2090) and from that time to the end of the curves. Karion Instant, however, is an exception: while the parameter values from the rotary machine are similar to those of Vivacel, this material displays much higher plasticity as expressed by the area quotient from the eccentric machine.

4.4.6. t_{off} and t_{diff}

A very good correlation exists between the times for the maximum forces and the time for minimum edge height (E XI) and the middle of t_{dwell} (PT 2090), where Karion Instant again is an exception: the value for Karion Instant from the PT 2090 is much higher than would be expected from the results with the E XI (Fig. 12). On the rotary machine, relaxation during t_{dwell} strongly affects t_{off}; an effect already during the compression phase preceding t_{dwell} time would hardly be detected. Thus, the start of t_{dwell} represents the lower limit for the occurance of F_{max}. There is no such limit on the eccentric machine. Since the rate of densification gradually decreases over a long time period (Fig. 4),

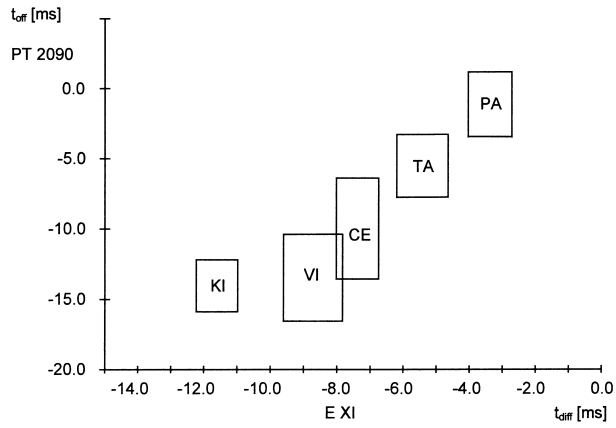

Fig. 12. Peak-offset times, t_{off}, of force/time curves on the Fette PT 2090 rotary machine (20 rpm), correlated to the time differences, t_{diff}, between time of F_{max} and s_{min} on the Fette E XI eccentric machine (46.3 rpm) from tabletting different materials (symbols see Table 1) to an F_{max} of 3 kN; confidence limits ($P_{0.05}$) of the means.

relaxation may occur during a long part of the force/time curve.

5. Conclusions

The main value of the rotary tabletting machine for evaluating the tabletting behavior of powders seems to be the registration of the force/time curve during the dwell time, which by its degree of assymmetry may serve to quantify the extent of plastic deformation. In addition, the modern rotary machine used provided real 'process conditions' for high-speed production with regard to the velocity of the punches, which modifies the extent of rate-depending processes, namely visco-elastic and plastic deformation.

However, this rotary press used did not fulfil the requirements of an analytical instrument at high rotation speeds. Certain parts between the tablets' surface and the load cell are not stiff enough for the high total mass of these parts, causing a bouncing of the force signal. This effect precluded the evaluation of the elastic recovery under load. With an eccentric tabletting machine, differing mechanism of densification can lead to similar force/time curves, resulting in similar parameter values, e.g. of the modified Weibull function.

In conclusion, the results from both machines with respect to the densification behavior complement one another.

A well instrumented, smaller and slower rotary machine may well be sufficient for such purpose, since by modification of the pressure roll and of the curvature of the punch heads a wide range of dwell times may be accomplished, as was already proposed by Vogel [19].

Acknowledgements

We like to thank the Wilhelm Fette GmbH, especially Mr Schiller and Mr Bomrowitz, for the opportunity to use their most advanced production machine, Mrs Petra Belda for very skilful help in the tabletting experiments, and the companies Rettenmaier, E. Merck, Meggle, and Parmentier for generous supply of excipients.

References

[1] F.X. Muller, L.L. Augsburger, The role of the displacement–time waveform in the determination of Heckel behaviour under dynamic conditions in a compaction simulator and a fully-instrumented rotary tablet machine, J. Pharm. Pharmacol. 46 (1994) 468–475.

[2] P. Ridgway Watt, Tablet Machine Instrumentation in Pharmaceutics, Principle and Practice, Ellis Horwood, Chichester, 1988.

[3] R.W. Heckel, Density-pressure relationships in powder compaction, Trans. Metall. Soc. AIME 221 (1961) 671–675.

[4] F. Müller, Viscoelastic models, in: G. Alderborn, C. Nyström (Eds.), Pharmaceutical Powder Compaction Technology, Marcel Dekker, New York, 1996, pp. 99–132.

[5] R. Dietrich, J.B. Mielck, Parametrisierung des zeitlichen Verlaufs der Verdichtung bei der Tablettierung mit Hilfe der modifizierten Weibull-Funktion, Pharm. Ind. 46 (1984) 863–869.

[6a] P. Konkel, J.B. Mielck, A compaction study of directly compressible vitamine preparations for the development of a chewable tablet, Pharm. Technol. 16 (3) (1992) 138–146.

[6b] P. Konkel, J.B. Mielck, A compaction study of directly compressible vitamine preparations for the development of a chewable tablet, Pharm. Technol. 16 (5) (1992) 42–54.

[7] J.B. Mielck, G. Stark, Tabletting of powder mixtures: parameters of evolved pressure–time profiles indicate percolation thresholds during tabletting, Eur. J. Pharm. Biopharm. 41 (1995) 206–214.

[8] G. Shliehout, G. Zessin, Investigation of the mechanical properties of different pharmaceutical excipients during compression by use of the Fraser–Susuki function and the thermal-mechanical analysis, Eur. J. Pharm. Biopharm. 42 (1996) 9S.

[9] D. Schierstedt, F. Müller, Rückdehnung und Relaxation während der Tablettierung mit Exzentermaschinen, Pharm. Ind. 44 (1982) 932–937.

[10] R.N. Chilamkurti, C.T. Rhodes, J.B. Schwartz, Some studies on compression properties of tablet matrices using a computerized instrumented press, Drug Dev. Ind. Pharm. 8 (1982) 63–86.

[11] B. Emschermann, F. Müller, Auswertung der Kraftmessung beim Tablettieren, Pharm. Ind. 43 (1981) 191–194.

[12] P.C. Schmidt, S. Ebel, H. Koch, T. Profitlich, U. Tenter, Preßkraft- und Weg-Zeit-Charakteristik von Rundlauftablettenpressen—4. Mitt.: Quantitative Auswertung von Preßkraft-Zeit-Kurven, Pharm. Ind. 50 (1988) 1409–1412.

[13] P.C. Schmidt, H. Koch, Zur Auswertung von Preßkraft-Zeit-Kurven, Eur. J. Pharm. Biopharm. 37 (1991) 7–13.

[14] P.J. Vogel, P.C. Schmidt, Force–time curves of a modern rotary tablet machine. II: Influence of compression force and tabletting speed on the deformation mechanisms of pharmaceutical substances, Drug Dev. Ind. Pharm. 19 (1993) 1917–1930.

[15] R.J. Oates, A.G. Mitchell, Calculation of punch displacement and work of powder compaction on a rotary tablet press, J. Pharm. Pharmacol. 41 (1989) 517–523.

[16] S.K. Dwivedi, R.J. Oates, A.G. Mitchell, Peak offset time as an indicator of stress relaxation during tabletting on a rotary press, J. Pharm. Pharmacol. 43 (1991) 673–678.

[17] K.M. Picker, Hydrophile Matrixtabletten: Tablettierung und Freisetzung unterer besonderer Berücksichtigung der relativen Feuchte während der Herstellung, Dissertation, Hamburg, 1995.

[18] P. Konkel, Untersuchungen zur Vergleichbarkeit von Parametern der Tablettierbarkeit pharmazeutischer Haufwerke an Exzenter- und Rundlauf-Tablettiermaschinen, Dissertation, Hamburg, 1995.

[19] P.J. Vogel, Charakterisierung des Verformungsverhaltens von Tablettierhilfsstoffen mit einer Hochleistungs-Rundlaufpresse unter praxisnahen Bedingungen, Dissertation, Tübingen, 1992.

[20] C. Führer, Über den Druckverlauf bei der Tablettierung in Exzenterpressen, Dtsch. Apoth. Ztg. 102 (1962) 827–832.

[21] J.R. Hoblitzel, C.T. Rhodes, Determination of a relationship between force–displacement and force–time compression curves, Drug. Dev. Ind. Pharm. 16 (1990) 201–229.

[22] P. Paronen, J. Ikka, Porosity-pressure functions, in: G. Alderborn, C. Nyström (Eds.), Pharmaceutical Powder Compaction Technology, Marcel Dekker, New York, 1996, pp. 59–60.

[23] A.Y.K. Ho, T.M. Jones, Punch travel beyond peak force during tabletting, J. Pharm. Pharmacol. 40 (1988) 75P.

[24] P. Belda, J.B. Mielck, The tabletting behaviour of Cellactose® compared with mixtures of celluloses with lactoses, Eur. J. Pharm. Biopharm. 42 (1996) 325–330.